Eksplorium
Volume 46 No. 1, May 2025: 59–68

p-ISSN 0854-1418
e-ISSN 2503-426X

Adsorption of Uranium onto Delaminated Amino Talc-Like Clay

Dwi Luhur Ibnu Saputra[1,2], Henny Purwaningsih[1*], Muhammad Farid[1], Triyono Basuki[2*], Satoru Nakashima[3], Jaka Rachmadetin[2], Roza Indra Laksmana[2], Juan Carlos Sihotang[2], Erlina Noerpitasari[2]

[1]Department of Chemistry, IPB University
Dramaga Raya St., Bogor, Jawa Barat 16680, Indonesia
[2]Research Center for Nuclear Material and Radioactive Waste Technology,
Research Organization for Nuclear Energy, National Research and Innovation Agency (BRIN)
B.J. Habibie Science and Technology Park, Tangerang Selatan, Banten 15314, Indonesia
[3]Graduate School of Advanced Science and Engineering, Hiroshima University,
Kagamiyama, Higashi-Hiroshima, Hiroshima 739-8526, Japan
*E-mail: triy019@brin.go.id

Article received: 23 April 2025, revised: 25 May, accepted: 31 May 2025
DOI: 10.55981/eksplorium.2025.12316

ABSTRACT

Uranium-containing waste is generated as a by-product of nuclear power plants, radioisotope production, nuclear fuel fabrication, and mineral processing. A radioactive waste treatment plant treats radioactive liquid waste using various methods, including evaporator technology, ion exchange resins, and adsorbents. Various adsorbents have been investigated for the removal of uranium from aqueous solutions. Negatively charged adsorbents, such as natural clay, biomass-based adsorbents, and polymers, have been utilized for uranium adsorption. Previous research on uranium adsorption by amino clay, which has a positively charged surface, was still very limited compared to other adsorbents. In the present study, the application of Delaminated Amino talc-like Clay (DAC) for removing uranium from aqueous solutions was examined. DAC with amino propyl on the tetrahedral sheet surface is easily protonated to form a positively charged R-NH_3 that may influence its interaction with uranium. The speciation and reaction kinetic order were studied in aqueous solution with pH and contact time as the variables. The adsorption of uranium onto DAC, which is likely due to physicochemical interactions and ion trapping, was evaluated. The maximum removal efficiency (84.5%) and adsorption capacity (113.06 mg/g) were achieved at pH 4 after approximately 60 minutes. The uranium adsorption capacity is low at pH 2 and 3 (10%), which is due to the repulsive interaction between the positive surface charge of DAC and $(UO_2)^{2+}$ as the dominant uranium species. Uranium adsorption capacity is high at pH 4 and 5, because the predominant species of uranium, such as $(UO_2)^{2+}$ and $[(UO_2)_2(OH)_2]^{2+}$, were probably adsorbed by DAC through chemisorption with R-NH_2. The adsorption of uranium on the DAC was found to follow the pseudo-second order kinetic model.

Keywords: delaminated talc-like amino clay, uranium adsorption, pH dependency, kinetic model

INTRODUCTION

Uranium waste is a by-product of nuclear power plants, radioisotope generation, nuclear fuel production, and mineral processing [1], [2]. This type of waste contains radioactive materials that pose significant risks to human health and the environment. Consequently, implementing proper waste management and treatment strategies is essential to prevent long-term contamination and ensure environmental safety.

Radioactive liquid waste is commonly treated using evaporation, ion exchange resins, and adsorption techniques [3], [4]. The acceptability of liquid waste that can be treated must follow established criteria. Liquid radioactive waste must be free from corrosive solvents, have a maximum chloride ion

content of 0.1 g/L, and have a pH > 7 [5]. However, radioactive liquid waste containing uranium is typically acidic, which can limit the effectiveness of treatment methods such as evaporation, ion exchange resins, or adsorption [5]. Therefore, the treatment of acidic liquid waste containing uranium is still being researched.

The treatment of liquid waste can be carried out using several methods, one of which is the adsorption method. Many types of adsorbents have been used for uranium adsorption. Functional organics such as methyl(3)-O-acetyl-5,6-dideoxy-(S)-1,2-trichloroethylidene-R-D-xylo-hept-5(E)-eno-1,4-furano-uronate and catechol diazotized aminopropyl silica gel, polymer embedded with oleic acid coated Fe_3O_4, pillar(5)arene-containing porous organic polymers have been used for the adsorption of aqueous uranium [6], [7]. Furthermore, negatively charged adsorbents such as natural clay, biomass-based adsorbents, and polymers have been utilized for uranium adsorption. On the other hand, previous research on uranium adsorption by positively charged adsorbents, such as amino talc-like clay, was still very limited compared to other adsorbents [8]. The positively charged adsorbent is effective in adsorbing uranium in the negatively charged speciation at pH levels greater than 3.

Amino talc-like clay is a positively charged synthetic clay that is produced using a variety of amino functional silane as precursor with a variety of different organosiloxanes, including methyltrihoxysilane, phenyltriethoxysilane, 3-mercaptopropyl) trimethoxysilane (APTES), 3-aminopropyl)-triethoxysilane, and 3-(methacryloxy) propyltrimethoxysilane [9]. These materials have been created in a novel manner, and Delaminated Amino talc-like Clay (DAC) is one of the desired structures that have been synthesized [10]. The chemical formula of magnesium-amino clay, which contains magnesium, is $Mg_3(RSi)_4O_8(OH)_{2.2}N(CH_2)_3]_8$ $Si_8Mg_6O_{16}(OH)_4$, where $[H_2N(CH_2)_3]_8$ is R and belongs to the organic group [11]. The NH_2-containing organic groups are covalently bound to silicon atoms on the tetrahedral sheet. Group $-NH_2$ on the surface of magnesium amino clay of tetrahedral sheets is easily protonated into positively charged $-NH_3$ [11], [12]. Amino clay has a nanoparticle to micro-particle size range of 0.1–10 μm, which is a schematic representation of the size of the smectite layer [13]. The schematic formation of DAC by the sol-gel process is shown in Figure 1 [14].

In this study, a synthetic delaminated amino talc-like clay was used as an adsorbent for uranium for the first time, without the addition of an anionic ligand. The purpose of this study is to evaluate the effect of pH variation (2~5) and to determine the adsorption kinetic model of uranium adsorption using DAC.

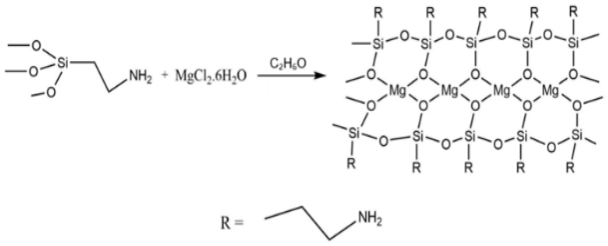

Figure 1. Schematic reaction for the formation of DAC

METHODOLOGY

Chemicals and Reagents

All the uranium solutions were prepared by dissolving uranyl nitrate hexahydrate $[UO_2(NO_3)_2.6H_2O]$, (pro-analys). The amino talc-like clay precursor included $H_2N(CH_2)_3Si(OC_2H_5)_3$ (APTES) and $MgCl_2.6H_2O$. Ethanol, 99%, is used as a solvent. HNO_3 is used for pH adjustment.

p-ISSN 0854-1418
e-ISSN 2503-426X

Synthesize DAC

The sol-gel aminopropyl method was performed following the previous method [15]. A magnesium chloride solution was prepared by dissolving 1.692 g of ($MgCl_2.6H_2O$) in 40 mL of ethanol while stirring at room temperature, approximately 298 K. Then, 0.015 mol of APTES was added dropwise, the solution was stirred overnight, and a white suspension was obtained. The suspension was centrifuged at 3500 rpm for 5 minutes, and the precipitate was washed with 40 mL of ethanol. The precipitate was then vortexed for 1 minute and centrifuged to remove the washing solution. The white precipitate was oven-dried at 323 K for approximately 5 days [15].

Characterization

The synthesized materials were characterized by Fourier Transform Infrared (FTIR) spectrometry (Bruker), Powder X-ray Diffraction pattern (P-XRD) analysis (PAN analytical) was acquired using Cu Kα radiation, X-Ray Fluorescence (XRF) spectrometry (S2 PUMA-Bruker), and Scanning Electron Microscopy (SEM) with Energy Dispersive X-Ray Analysis (EDS) (Phenom Pharos). The P-XRD analysis (PAN analytical) is employed to determine the crystallographic and amorphous structures of materials [16], and it was acquired using Cu Kα radiation, with a 2θ range of 5−80°, at room temperature. FTIR analysis is employed to determine the presence of specific functional groups in the sample. XRF analysis is utilized to determine major elemental composition. SEM-EDS analysis is used to analyze the surface morphology of the sample.

Batch Adsorption Experiments

Experiments were performed at room temperature in a batch system. In all experiments, a 53 mg/L uranium solution (25 mL, pH 2~5), and Mg-amino clay adsorbent 0.001 g were used [3]. The mixture was shaken using an orbital shaker (Daihan Scientific) at an agitation speed of approximately 170 rpm. The mixture was centrifuged to separate the supernatant from the adsorbent. The concentration of uranium ions in the supernatant solution was determined by UV/Vis Spectrophotometer using arsenazo III as a complexing agent with light adsorbent maximum (λ) at 651 nm [17].

Some equations for calculating uranium adsorption by DAC include removal efficiency, adsorption capacity, and the kinetic adsorption model. The removal efficiency was calculated using the following equation [3]:

$$Removal\ Eff(\%) = \frac{(C_o - C_e)}{C_o} x\ 100 \qquad (1)$$

where C_o is the initial concentration of uranium (mg/L), and C_e is the equilibrium concentration of uranium after adsorption (mg/L). The adsorption capacity was calculated using the following equations [18]:

$$q_e = (C_o - C_e) x \frac{V}{m} \qquad (2)$$

where V is the volume of solution (L) and m is the weight of the DAC (g). The kinetics experimental data were simulated using pseudo-first order as follows [19]:

$$\log(q_e - q_t) = \log q_e - \frac{k_1}{2.303} t \qquad (3)$$

and pseudo-second order models using the equation as follows [19]:

$$\frac{t}{q_t} = \frac{1}{k_2 q_e^2} + \frac{1}{q_e} t \qquad (4)$$

RESULTS AND DISCUSSION

DAC Characterization

The P-XRD pattern of DAC before and after uranium adsorption is given in Figure 2. The characteristic peaks of DAC before Adsorption were observed at 2θ = 6.11°, 10.79°, 22.00°, 36.76°, and 59.29°. In general, based on the P-XRD pattern, the sample exhibits broad peaks corresponding to an amorphous phase. The pattern is consistent with the P-XRD pattern of amino clay reported in a previous study [14]. The change of the P-XRD pattern after uranium adsorption was observed (Figure 2). After uranium adsorption, the P-XRD pattern of DAC exhibits a notable decrease in peak intensity, particularly in the low-angle region. This may imply partial hydrogen bond breaking between the amino clay sheets as a result of the interaction between the -NH_2 group and uranium species, leading to a crystal defect. The concentration of uranium species $[UO_2]^{2+}$, $[(UO_2)_2(OH)_2)]^{2+,}$ probably induced the exfoliation of DAC, and the surface of exfoliated DAC was filled up with uranyl and uranyl hydroxide. The exfoliation of DAC can be examined based on the left-shifting of the diffraction peak at low angles associated with the (001) plane. The calculated d-spacing of the (001) plane was slightly increased from 1.45 nm to 1.71 nm, which is probably due to the presence of uranyl species at the interlayer space of the DAC.

FTIR

The FTIR analysis result is given in Figure 3. DAC before uranium adsorption shows IR absorption at wavelength corresponded to the C-H *stretching* and C-H bending (3043.07, 2933.31, 1468.33, 1387.29 cm^{-1}), H bonded at group -OH (3358.76), NH_3^+ (1619 and 1627 cm^{-1}), NH_2 (1506 and 1497 cm^{-1}), Si–O–Si (1125 cm^{-1}), Si–OH (994.7 and 996.67 cm^{-1}), Mg–O–Si (842 and 881 cm^{-1}), Mg–O (559 and 547 m^{-1}) [14], [20]. After uranium adsorption, the IR spectra show no peak at the wavenumbers corresponding to OH, -CH, and -NH, and the appearance of a new band that probably corresponds to the uranium–NH_2 bond (Figure 3). Infrared absorption spectra of the uranium-nitrogen bond have been reported previously at 3349.7, 966.9, 752.4, and 433.0 cm^{-1} [21].

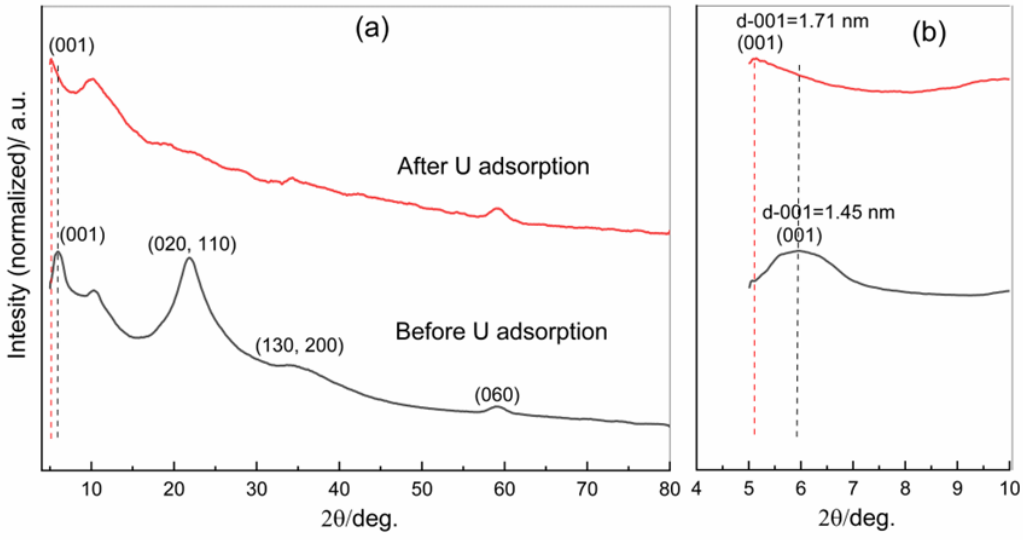

Figure 2. PXRD pattern of DAC before and after uranium adsorption

p-ISSN 0854-1418
e-ISSN 2503-426X

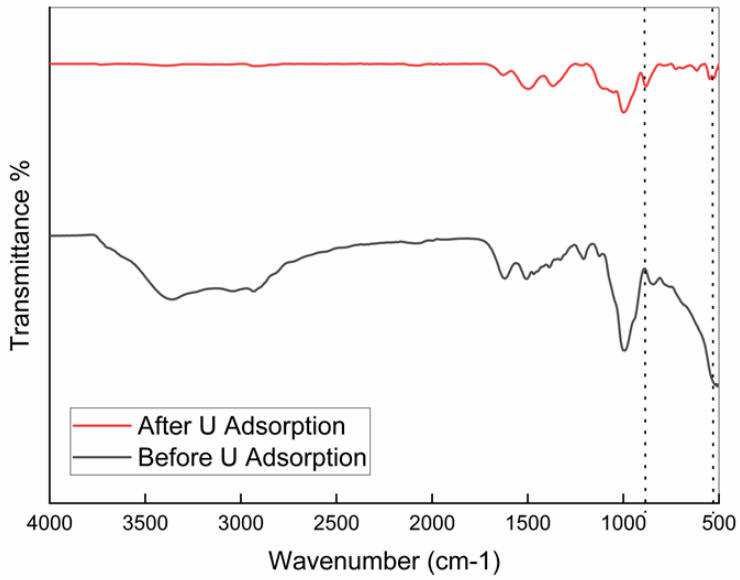

Figure 3. FTIR pattern of DAC before and after uranium adsorption

XRF

Table 1 shows the XRF analysis result. The analysis was carried out using the precipitated DAC derived from the optimum condition of the uranium adsorption experiment, which was conducted for 24 hours. XRF analysis reveals that the major elements of DAC are Cl, Mg, and Si. Other elements contained impurities that did not originate from the DAC adsorption material. The presence of uranium was observed in the DAC particle after uranium adsorption and was dominant over other elements (Table 1). It was strong evidence of the uranium adsorption by DAC.

Table 1. Major elemental composition of particles DAC based on XRF spectroscopy

Elements	Concentration of Elements	
	Before adsorption (%)	After adsorption (%)
Cl	23.70	0.60
Mg	24.10	12.60
Si	15.50	8.00
U	0.00	45.30

SEM

The SEM images, along with the EDS spectra, of the DAC before and after uranium adsorption are illustrated in Figure 4. The morphology of the DAC before uranium adsorption consisted of homogeneous particles with a grain size of approximately 0.5 µm, as shown in Figure 4a. The EDS spectra show the presence of O, Mg, and Si, which is in line with the components of magnesium phyllosilicate clay. Figure 4b presents the SEM image of DAC and EDS spectra after uranium adsorption. The SEM image exhibits large aggregate particles, which are very different from the original DAC particle. It may indicate that uranium adsorption causes the aggregation of DAC particles. White spots observed on the particle surface likely indicate the deposition of uranium [22]. Moreover, the presence of uranium adsorbed by DAC is confirmed based on SEM-EDS spectra spots 1 and 2 (Figure 4b).

p-ISSN 0854-1418
e-ISSN 2503-426X

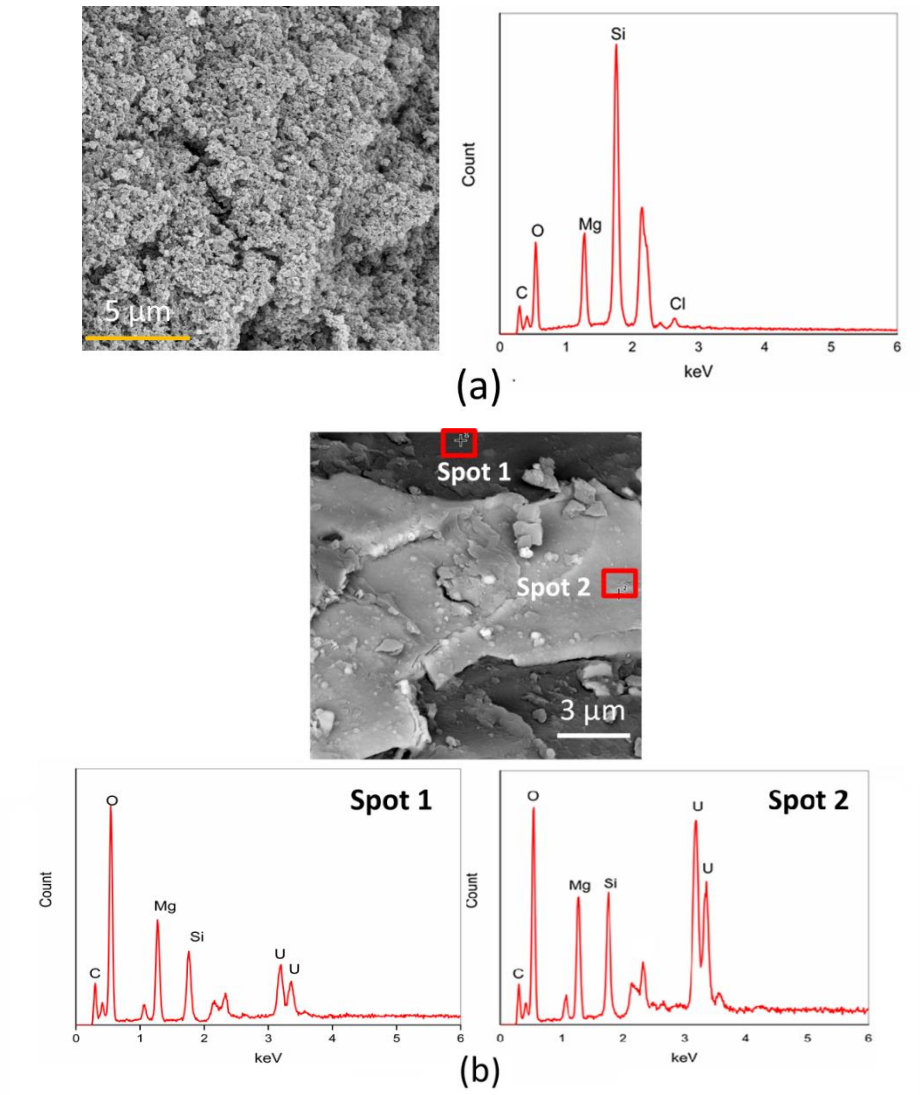

Figure 4. SEM image and EDS spectra of DAC before (a) and after (b) uranium adsorption

Effect of Initial pH Solution

The uranium adsorption onto DAC at different pH levels is presented in Figure 5. The effect of pH (2~5) on uranium adsorption by DAC was obvious. The effect of the pH solution was clearly demonstrated at pH 4, with a removal efficiency of 95%. A combination of physicochemical interactions and ion-trapping processes likely governs the adsorption mechanism. The trapping of $(UO_2)^{2+}$ ions in the basal spacing occurs due to the repulsive interaction between the $(UO_2)^{2+}$ ions, which are the predominant species at acidic pH 2 and 3, and the positively charged surface of DAC. Ligand R-NH_2 on the surface was protonated at pH 2 and 3 to form colloids. The interlayer spaces in DAC functioned as trap containments, which are known to have high swelling capacity [23]. The cesium ion trapping phenomenon, leading to the formation of CsCl particles, has been previously reported [15]. On the other hand, predominant species at acidic pH levels of 4 and 5, such as $(UO2)^{2+}$ and $[(UO_2)_2(OH)_2]^{2+}$ [24], predicted by Minteq Visual software (Figure 6), were probably adsorbed by DAC through chemisorption with R-NH_2. Illustrations of the ion trapping mechanism and chemisorption are shown in Figures 7 and 8, respectively.

p-ISSN 0854-1418
e-ISSN 2503-426X

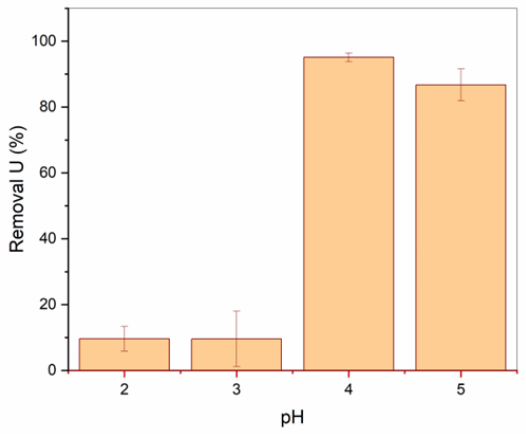

Figure 5. Effect of initial pH solution for uranium adsorption onto DAC

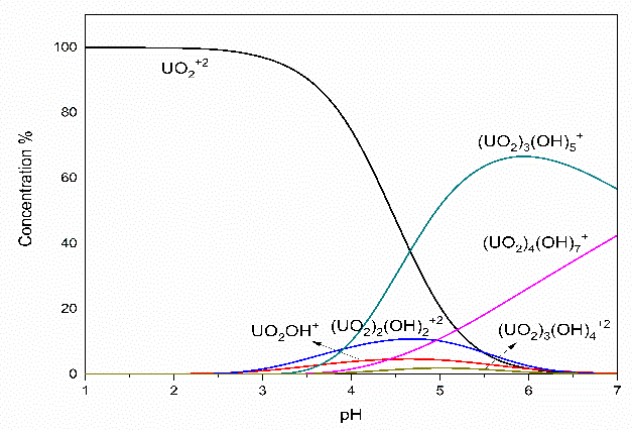

Figure 6. Uranium speciation in aqueous solution at different pH levels without ligand predicted using Minteq Visual software

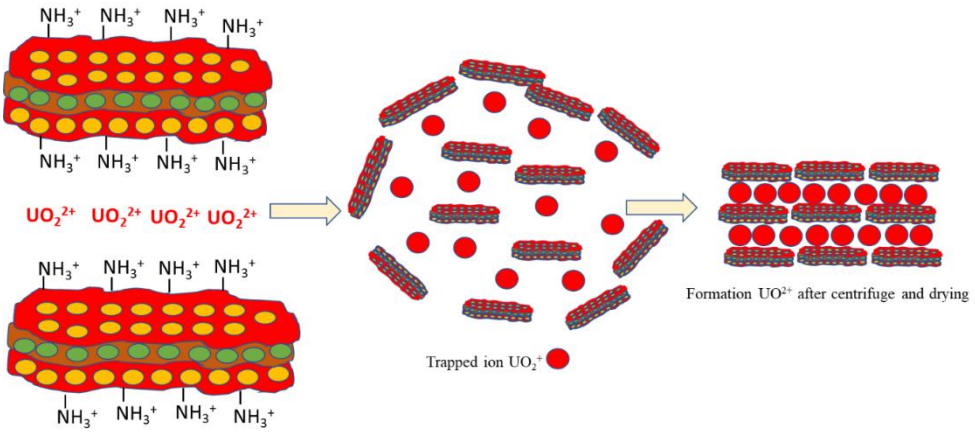

Figure 7. Schematic of the ion trapping mechanism of uranium at pH 2 and 3

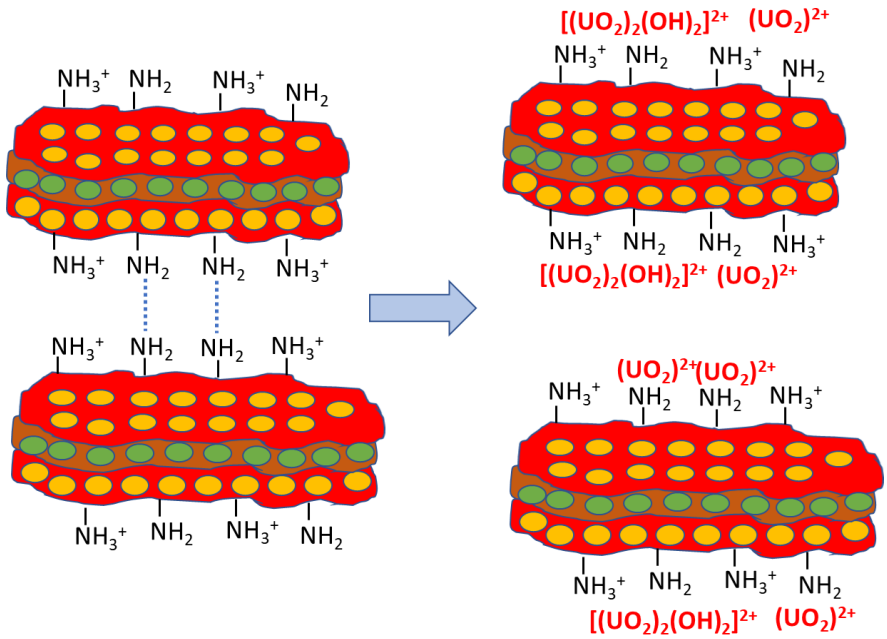

Figure 8. Schematic chemisorption mechanism of uranium adsorption at pH 4 and 5

Adsorption Kinetics

Adsorption kinetics provides important insights into the mechanism governing the adsorption process, which in turn controls residence time and mass transfer [25]. The adsorption equilibrium has been reached after 60 minutes, where the removal efficiency of uranium was 84.5 % (Figure 9) and the adsorption capacity (q_e) at equilibrium was 113.06 mg/g (Figure 10).

The results of the experiment have been plotted based on the pseudo-first-order kinetic model of $log\ (q_e - q_t)$ vs t were used to determine the values of k_1 and q_e, from the slope and intercept. Pseudo-second-order models with plots of $\frac{t}{q_t}$ vs t were used to determine the values of k_1 and q_e, from the slope and intercept. The results of determining models for pseudo-first-order and pseudo-second-order adsorption from equilibrium are presented in Table 2. The model represented from these results is the linear pseudo-second-order kinetic model because experimental values q_e are almost similar to a q_e linear regression calculation where its value is close to 1. The graph of the model is presented in Figure 11.

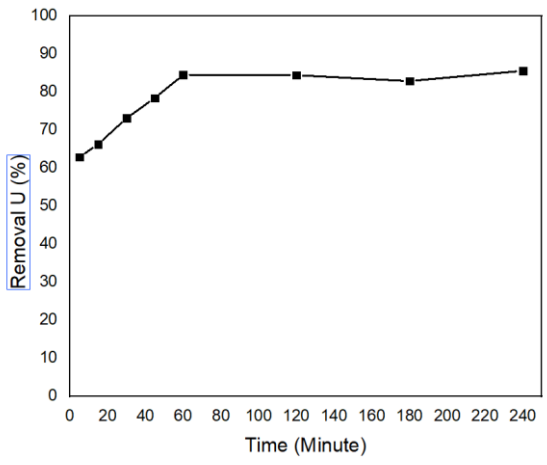

Figure 9. Adsorption kinetic of uranium onto DAC

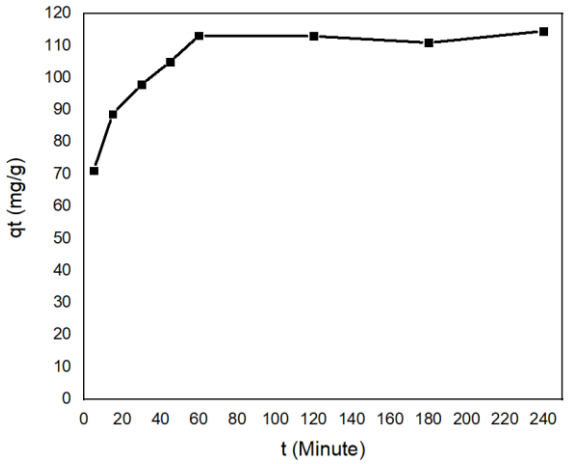

Figure 10. Adsorption equilibrium from adsorption capacity of uranium onto DAC

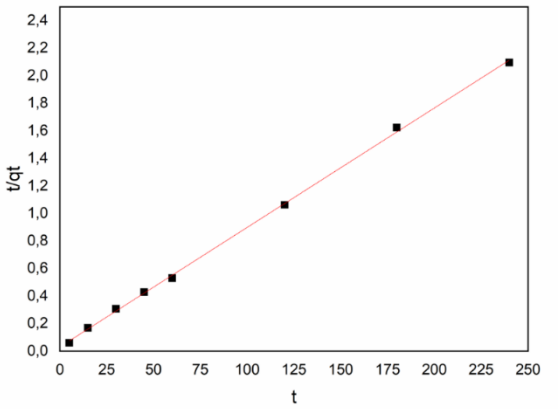

Figure 11. Pseudo-second order kinetics of uranium adsorption onto DAC

Table 2. Models of pseudo-first-order and pseudo-second-order from the adsorption equilibrium

Value	Models	
	Pseudo-first-order	Pseudo-second-order
$q_{e\ exp}$ (mg/g)	113.06	113.06
$q_{e\ cal}$ (mg/g)	36.85	108.7
$\frac{K_1}{K_2}$ (1/min)	0.0320117	0.00368
R^2	0.977	0.999

CONCLUSION

This work confirmed the occurrence of uranium adsorption onto DAC, which is probably due to physicochemical interactions and ion trapping. The uranium adsorption on DAC can be clearly observed based on the sample characterization (XRF and SEM EDS

p-ISSN 0854-1418
e-ISSN 2503-426X

analysis) of DAC after uranium adsorption. Uranium adsorption was affected by different pH and contact time. Adsorption probably occurs due to physicochemical interactions and ion trapping. The phenomenon of $(UO_2)^{2+}$ ion trapping in basal space, because of the repulsive interaction between $(UO_2)^{2+}$ ion as the predominant species at acidic pH 2 and 3, with positive surface charge of DAC.

On the other hand, predominant species at acidic pH levels of 4 and 5, such as (UO2)2+ and $[(UO_2)_2(OH)_2]^{2+}$, were probably adsorbed by DAC through chemisorption with R-NH_2. The removal efficiency and adsorption capacity at equilibrium are approximately 84.5% and 113.06 mg/g, respectively, which are reached at pH 4 and approximately after 60 minutes. The pseudo-second-order model can well describe the adsorption kinetics. These findings highlight DAC as a promising material for treating uranium-containing waste, with implications for the treatment of radioactive waste.

ACKNOWLEDGMENT

This work is financially supported by the Grant for Research and Innovation for Indonesia Advancement (RIIM) from the LPDP Ministry of Finance and the National Research and Innovation Agency (BRIN) of Indonesia, grant no. 37/II.7/HK/2023, as well as the Nuclear Technology Innovation Results (HITN) of the National Research and Innovation Agency (BRIN). The facilities and scientific and technical support from the Advanced Characterization Laboratories in Serpong, National Research and Innovation Agency, through E-Layanan Sains, BRIN, for PXRD, FTIR, XRF, and SEM analysis. We express our gratitude to the Research Organization for Nuclear Energy (ORTN) and BRIN for their administrative support and funding for this study.

REFERENCES

[1] H. Ma, M. Shen, Y. Tong, and X. Wang, Radioactive Wastewater Treatment Technologies: A Review," *Molecules*, vol. 28, no. 4. MDPI, Feb. 2023, doi: 10.3390/molecules28041935.

[2] D. Vopálka, K. Štamberg, A. Motl, and B. Drtinová, "The study of the speciation of uranyl-sulphate complexes by UV-Vis absorption spectra decomposition," J. Radioanal. Nucl. Chem., vol. 286, no. 3, pp. 681–686, 2010, doi: 10.1007/s10967-010-0764-5.

[3] D. Luhur Ibnu Saputra et al., "Urania Jurnal Ilmiah Daur Bahan Bakar Nuklir Adsorpsi Uranium Menggunakan Na Dan Zr-Montmorillonite," *J. Ilm. Daur Bahan Bakar Nukl.*, vol. 29, no. 2, pp. 105–114, 2023, doi: 10.17146/urania.2023.29.2.6979.

[4] M. Jiménez-Reyes, P. T. Almazán-Sánchez, and M. Solache-Ríos, "Radioactive waste treatments by using zeolites. A short review," *J. Environ. Radioact.*, vol. 233, 2021, doi: 10.1016/j.jenvrad.2021.106610.

[5] A. Setiawan, *Kriteria Keberterimaan Limbah Radioaktif Cair*, in: Dokumen Instalasi Pengelolaan Limbah Radioaktif (1st Ed.), National Research and Innovation Agency, Indonesia, 2022.

[6] M. A. A. Aslani, S. Yusan, N. Yenil, and S. Kuzu, "Sorption profile of uranium (VI) from aqueous medium onto 3-O-acetyl-(S)-1,2-O-trichloroethylidene-5,6,8-trideoxy-α-d-xylo-oct-5(E)-eno-1,4-furano-7-ulose (OASOTCETDOXDXOEEFU)," *Chem. Eng. J.*, vol. 200–202, pp. 391–398, 2012, doi: 10.1016/j.cej.2012.06.072.

[7] X. Zhao, Z. Liu, S. Zang, M. Hassan, C. Ma, Z. Liu, and W. Gong, "Synthesis of Pillar[5]arene- and Phosphazene-Linked Porous Organic Polymers for Highly Efficient Adsorption of Uranium," *Molecules*, vol. 28, no. 3, pp. 1–14, 2023, doi: 10.3390/molecules28031029.

[8] M. Solgy, M. Taghizadeh, and D. Ghoddocynejad, "Adsorption of Uranium(VI) from Sulphate Solutions using Amberlite IRA-402 Resin: Equilibrium, Kinetics and Thermodynamics Study," *Ann. Nucl. Energy*, vol. 75, pp. 132–138, Jan. 2015, doi: 10.1016/j.anucene.2014.08.009.

[9] S. L. Burkett, A. Press, and S. Mann, "Synthesis, Characterization, and Reactivity of Layered Inorganic-Organic Nanocomposites Based on 2:1 Trioctahedral Phyllosilicates," *Chem. Mater.*, vol. 4756, no. 7, pp. 1071–1073, 1997, doi: 10.1021/cm9700615.

[10] V. K. H. Bui, D. Park, and Y. C. Lee, "Aminoclays for biological and environmental applications: An updated review," *Chem. Eng. J.*, vol. 336, pp. 757–772, 2018, doi: 10.1016/j.cej.2017.12.052.

[11] R. Wang, G. Jing, X. Zhou, and B. Lv, "Removal of chromium(VI) from wastewater by Mg-aminoclay coated nanoscale zero-valent iron," *J. Water Process Eng.*, vol. 18, pp. 134–143, 2017, doi: 10.1016/j.jwpe.2017.05.013.

[12] G. P. Mendes, L. D. Kluskens, S. Lanceros-Méndez, and M. Mota, "Magnesium aminoclays as plasmid delivery agents for non-competent Escherichia coli JM109 transformation," *Appl. Clay Sci.*, vol. 204, 2021, doi: 10.1016/j.clay.2021.106010.

[13] E. A. Franco-Urquiza, "Clay-based polymer nanocomposites: Essential work of fracture," *Polymers (Basel).*, vol. 13, no. 15, 2021, doi: 10.3390/polym13152399.

[14] S. Badshah and C. Airoldi, "Layered organoclay with talc-like structure as agent for thermodynamics of cations sorption at the solid/liquid interface," *Chem. Eng. J.*, vol. 166, no. 1, pp. 420–427, 2011, doi: 10.1016/j.cej.2010.10.078.

[15] T. Basuki and S. Nakashima, "Cs Adsorption and CsCl Particle Formation Facilitated by Amino Talc-like Clay in Aqueous Solutions at Room Temperature," *ACS Omega*, vol. 6, no. 40, pp. 26026–26034, 2021, doi: 10.1021/acsomega.1c02975.

[16] R. Sharma, D. P. Bisen, U. Shukla, and B. G. Sharma, "X-ray diffraction: a powerful method of characterizing nanomaterials," *Recent Research in Science and Technology,* vol. 4, no. 8, pp. 77–79, 2012, [Online]. Available: https://updatepublishing.com/journal/index.php/rrst/article/view/933.

[17] H. Golmohammadi, A. Rashidi, and S. J. Safdari, "Simple and rapid spectrophotometric method for determination of uranium (vi) in low grade uranium ores using arsenazo (III)," *Chem. Chem. Technol.*, vol. 6, no. 3, pp. 245–249, 2012, doi: 10.23939/chcht06.03.245.

[18] A. M. Masoud, "Sorption behavior of uranium from Sulfate media using purolite A400 as a strong base anion Exchange resin," *Int. J. Environ. Anal. Chem.*, vol. 102, no. 13, pp. 3124–3146, 2022, doi: 10.1080/03067319.2020.1763974.

[19] X. Shi, Q. Li, T. Wang, and K. S. Lackner, "Kinetic analysis of an anion exchange absorbent for CO2 capture from ambient air," *PLoS One*, vol. 12, no. 6, Jun. 2017, doi: 10.1371/journal.pone.0179828.

[20] P. Gupta, S. S. Das, and N. B. Singh, *Introduction to spectroscopy*, in: Spectroscopy (1st Ed.), Jenny Stanford Publishing, New York, 2023, pp. 1–20.

[21] X. Wang, L. Andrews, B. Vlaisavljevich, and L. Gagliardi, "Combined triple and double bonds to uranium: The N≡U=N-H uranimine nitride molecule prepared in solid argon," *Inorg. Chem.*, vol. 50, no. 8, pp. 3826 – 3831, 2011, doi: 10.1021/ic2003244.

[22] E. Palamara, P. P. Das, S. Nicolopoulos, L. T. Cifuentes, A. Oikonomou, E. Kouloumpi, A. Terlixi, and N. Zacharias, "Applying SEM-Cathodoluminescence imaging and spectroscopy as an advanced research tool for the characterization of archaeological material," *Microchem. J.*, vol. 158, no. p. 105230, 2020, doi: 10.1016/j.microc.2020.105230.

[23] H. Li, S. Song, X. Dong, F. Min, Y. Zhao, C. Peng, and Y. Nahmad, "Molecular Dynamics Study of Crystalline Swelling of Montmorillonite as Affected by Interlayer Cation Hydration," *JOM*, vol. 70, no. 4, pp. 479–484, 2018, doi: 10.1007/s11837-017-2666-2.

[24] M. Zaky, A. E. M. Hussein, M. M. Fawzy, and K. Elgendy, "Removal of Uranium From Liquid Waste By Natural Nile Mud," *Bull. Fac. Sci. Zagazig Univ.*, vol. 2017, no. 2017, pp. 332–348, 2017, doi: 10.21608/bfszu.2017.31058.

[25] S. F. Azha, A. L. Ahmad, and S. Ismail, "Thin coated adsorbent layer: characteristics and performance study," *Desalin. Water Treat.*, vol. 55, no. 4, pp. 956–969, 2015, doi: 10.1080/19443994.2014.922502.